Particle Accelerators, 1992, Vols. 37–38, pp. 261–268
Reprints available directly from the publisher
Photocopying permitted by license only

A BEAM FUNNELLING DEMONSTRATION: EXPERIMENT AND SIMULATION*

K. F. JOHNSON, O. R. SANDER, G. O. BOLME, J. D. GILPATRICK, F. W. GUY,‡ J. H. MARQUARDT, K. SAADATMAND,† D. SANDOVAL and V. YUAN

Los Alamos National Laboratory, Los Alamos, NM 87545.

(Received 8 January 1991)

Accelerator concepts for heavy-ion fusion require small emittance, high-current beams. Such applications could include funnels in which high-current, like-charged particle beams are interlaced to double beam current while retaining small emittances. The first experimental demonstration confirming the beam dynamics of the funnel principle was recently completed at Los Alamos National Laboratory. A single-leg prototype 5-MeV H^- funnel was successfully tested. This single-beam demonstration explored physics issues of a two-beam funnel. It contained elements for emittance control, position control, and rf deflection, as well as diagnostics for measurement of beam intensity, position and angle centroids, energy and phase centroids, and transverse and longitudinal phase-space distributions. Results of the experiment will be presented along with comparisons to simulations.

An experimental demonstration confirming the beam dynamics of beam funnelling was recently completed on the Accelerator Test Stand (ATS)[1] at Los Alamos National Laboratory. Although this experiment utilized a single leg of a prototype 5-MeV H^- funnel, it addressed, with the exception of the beam-beam interaction, the physics issues concerned with a two-beam funnel. Objectives of this experiment were control of emittance growth, successful use of rf deflection, and position control (with $\sim 100\%$ beam transmission).

The funnel input beam was from the ATS H^-, 425-MHz, 5-MeV drift tube linac (DTL). The beam-line is shown schematically in Figure 1. Beam position control elements were four permanent-magnet dipoles (PMDs), four off-set, permanent-magnet quadrupoles (PMQs), four movable PMQs for steering, and one rf deflector. The beam dynamics design was by G. Taylor, R. Kashuba, K. Crandall and F. Guy.[2] Transverse and longitudinal emittance control were obtained with 15 PMQs and four rf bunchers (two 425-MHz and two 850-MHz), each with independent amplitude and phase control. A large cylindrical vacuum vessel contained the transport elements that were mounted on four separate plates (M1 through M4) to allow for staged installation. The 850-MHz bunchers and magnet mounts on the M3 plate extend into space that would be occupied by the second beamline in a two-beam funnel.

* Work supported and funded by the U.S. Department of Defense, Army Strategic Defense Command, under the auspices of the U.S. Department of Energy.

† Industrial partner, Grumman Corporate Research Center.

‡ Present Address: SSC Laboratory, Dallas, TX 75237

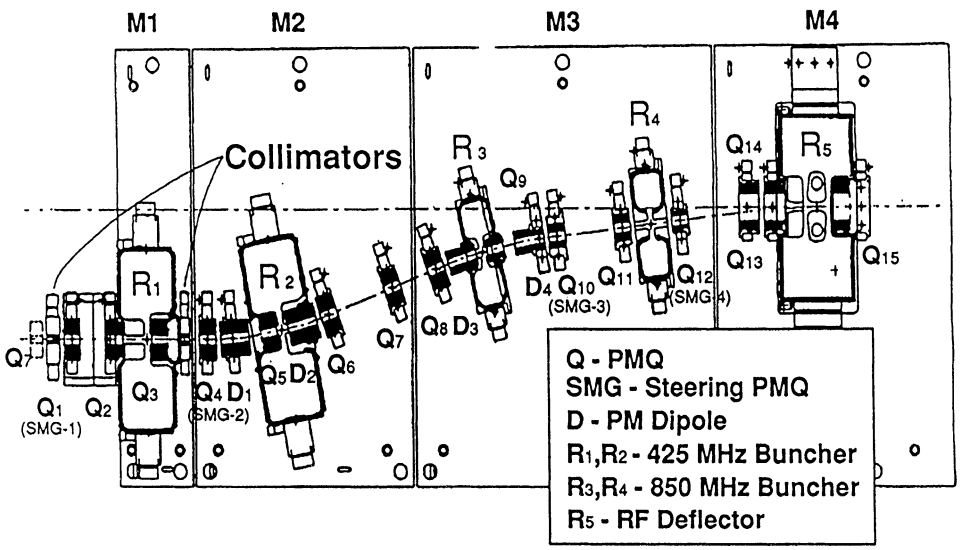

FIGURE 1 Funnel beamline schematic showing the locations of the optics elements.

These elements would be redesigned for a two-beam funnel (e.g. the bunchers would be quarter-wave-stub two-gap designs). The 850-MHz bunchers were used for compactness in this experiment. For beam dynamics, the choice of single-gap vs. two-gap bunchers make little difference, but frequency is important.

The funnel experiment was performed in four stages. These were the characterizations of the output beams from the DTL, M1, M3, and M4 plates. Beamline diagnostics included three broad-band toroids and nine microstrip probes (MBPs). Beam characterization diagnostics were mounted on a diagnostics plate (D-plate), which could be placed after each M plate. The diagnostics were two pairs of slit-collectors for transvere emittance measurements, the LINDA[3] (a longitudinal emittance measurement technique) intersection points, a sweeping magnet for longitudinal emittance measurements, three MBPs, one wide-band toroid, a beam stop, and a Faraday cup.

The rf amplitude and phase set-points of the DTL and R1 were determined using the phase-scan technique.[4,5] The phase-scan technique could not be used for cavities R2, R3, and R4 due to rf interference in the MBPs from the R1 cavity and the beam itself. Phase set-points for R2, R3, and R4 were determined by beam loading, and their amplitude set-points were determined by using LINDA to measure beam energy gain (checked with x-ray emission data[6]).

Longitudinal and transverse phase-space distributions of the DTL beam were characterized as a function of rf amplitude and phase. The transverse emittance in both planes had increased by a factor of 1.7 to 2.0, compared to previous measurements. Extensive instrument checks showed the increase to be real. To reduce the transverse emittance to an acceptable level for a meaningful physics test of the remainder of the funnel beamline (i.e. the M2 through M4 plates), two collimators

(movable vertically and horizontally) were installed on the M1 plate (at its entrance and exit).

The positions of the movable collimators and PMQ (SMG1) were optimized for beam injection into the M2 plate. The optimized positions were fixed for the duration of the experiment. The M1-plate beam transmission was $\sim 58\%$ with output currents between 25 to 40 mA. Phase-space distributions of the collimated beam were characterized, and the expected normalized transverse emittance was achieved ($\sim 0.021\ \pi$ cm-mrad in each plane).

Good transmission ($\sim 100\%$) through the M2- and M3-plates was achieved with the steering PMQs (SMG2–SMG4). These PMQs were used to adjust the beam position and angle centroids for injection into the M4 plate. The error on the transmission measurement was dominated by beam noise, not toroid measurement precision. For quiet beams, a relative uncertainty of $\sim 2\%$ on beam transmission measurements was possible.

The funnel steering model was verified, during characterization of the M3 plate output beam, by moving each SMG separately, vertically or horizontally, and measuring the changes in beam position and angle centroids at the funnel exit. Model and experiment agreed within measurement errors of ± 0.2 mm and ± 1 mrad.

Longitudinal and transverse phase-space distributions of the M3-plate output beam were measured for optimum settings of the four bunchers. To study sensitivities to non-optimum conditions, the measurements were repeated for other conditions (all buncher amplitudes decreased by 20%, all bunchers off, etc.) The normalized horizontal and vertical transverse emittances ε_x and ε_y were unchanged when the buncher amplitudes were decreased by 20% from their optimum settings.

RF deflector performance was critical to the success of the funnel experiment. Good transmission ($\sim 100\%$, 2% relative uncertainty) was achieved through the rf deflector with rf power "on" or "off". The horizontal beam deflection, the relative ε_x, ε_y, and ε_L were measured as functions of deflector phase and cavity power. The rf power set-point was determined from x-ray emission data. For 86 kW of power, x-ray data indicated a gap voltage of 333 ± 17 kV (design value 333 kV). Figures 2A and 3A show the dependence of the relative horizontal beam deflection and relative ε_x on the deflector phase. Both quantities show extremums at the same input phase. This behavior is repeated for the Courant–Snyder parameters α, β, and γ. The extrema in β and γ are related to minimization of position and angle spreads. The data give a clear signature for the rf phase set-point ($\sim 60^\circ$ relative phase) of the deflector. This phase was independent of cavity power (Figure 2A). Also, ε_y was independent of the deflector phase. These observations were as predicted. The behavior of ε_L with respect to deflector phase (Fig. 4A) is similar to that of ε_x. Although broader, its minimum occurs at approximately the same phase, as it should. Relative ε_x, ε_y, ε_L, and the Courant–Snyder parameters (in x and y) were shown to be independent of deflector cavity power. For power dependence of ε_x and ε_L see Figures 3B and 4B.

With the deflector set at its experimentally determined power and phase set-points, the measured absolute horizontal deflection of the beam was 36 ± 2 mrad. Simulations predicted a deflection of 38.4 mrad. Within the experimental error (~ 2 mr) and the 5% uncertainty in gap voltage, there was excellent agreement between measure-

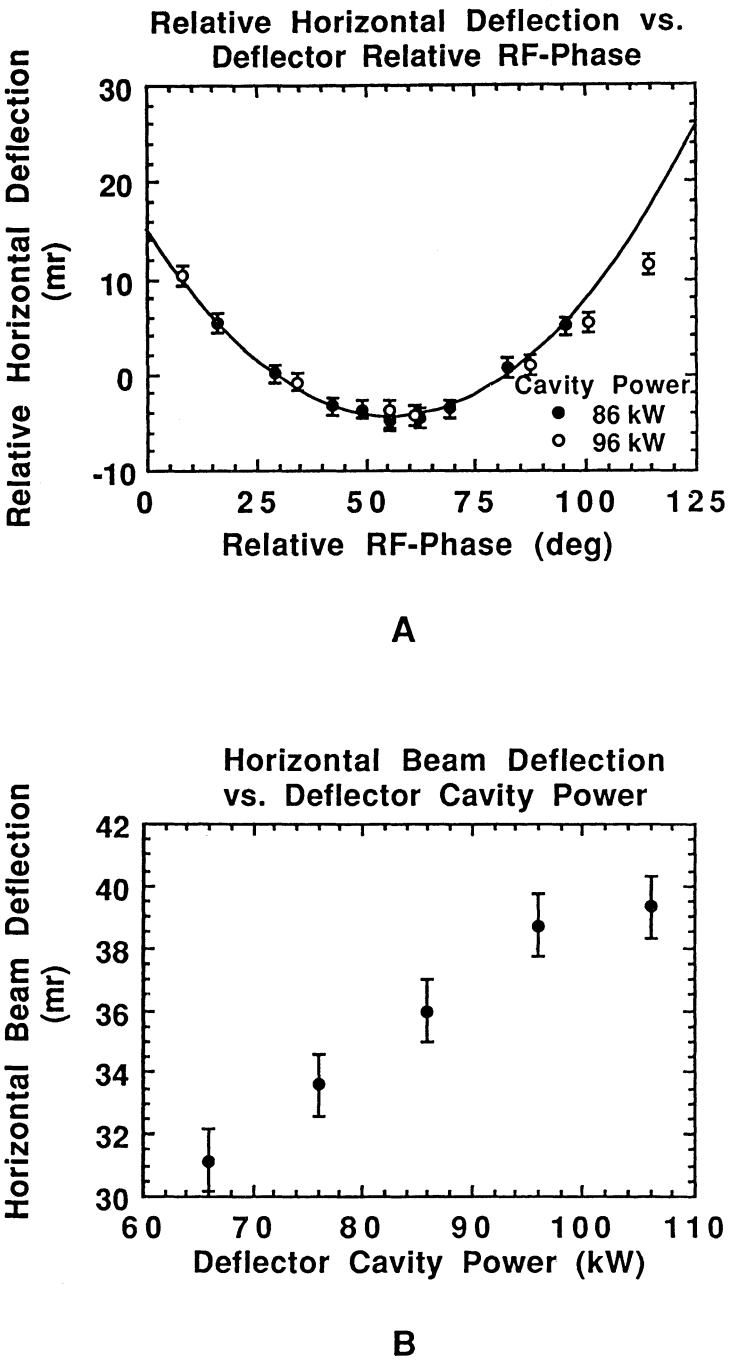

FIGURE 2 (A) Relative horizontal deflection angle of the deflector output beam vs. relative deflector phase. Data are shown for two deflector cavity power levels. The curve is to guide the eye. (B) Absolute horizontal beam deflection of deflector output beam vs. deflector power.

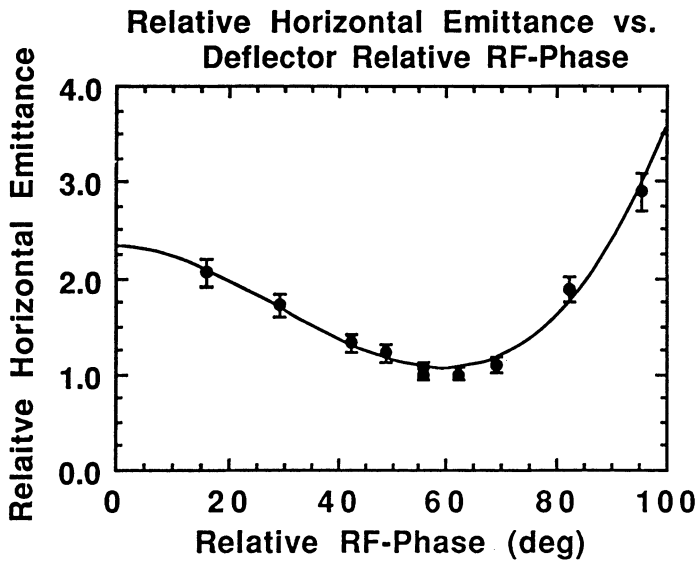

A

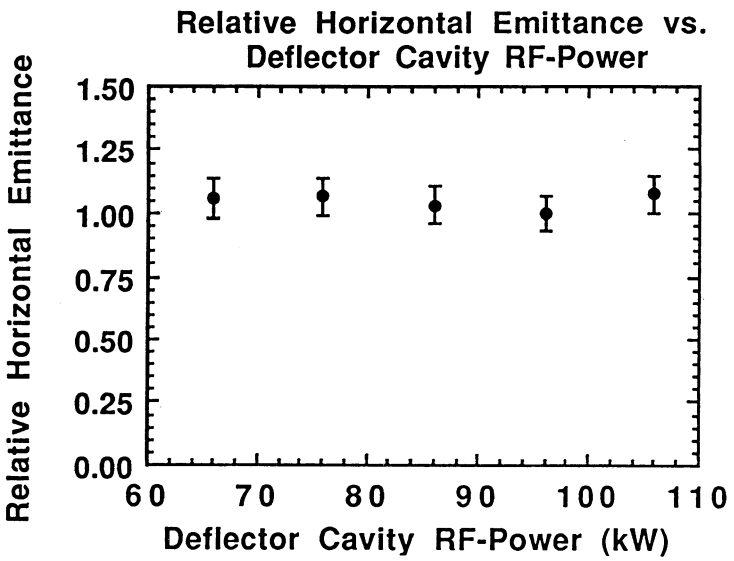

B

FIGURE 3 (A) Relative ε_x of the deflector output beam vs. relative deflector rf phase. Cavity power set at 86 kW. The curve is to guide the eye. (B) Relative ε_x of the deflector output beam vs. deflector rf power. Design gap voltage (333 kV) occurs at 86 kW.

ment and simulations. The beam deflection scaled with rf power as expected (Figure 2B).

With the bunchers and deflector at their optimum set-points, the transverse and longitudinal phase-space distributions were measured. Using the observed emittances and currents at the exit of the M1-plate as input to simulations, an upper limit of $\sim 5\%$ transverse emittance growth through the rest of the funnel beamline is predicted. Within experimental error, the data ($\varepsilon_x = 0.022\ \pi$ cm-mr and $\varepsilon_y = 0.020\ \pi$ cm-mr) are consistent with simulations and with no transverse emittance growth. The short-term and day-to-day reproducibility of the data is 2 to 3% and 8 to 10%, respectively. The error on the measurements is 5 to 8% with background subtraction being the dominant component.

An attempt to produce a measurable emittance growth with non-optimum buncher operation (amplitudes 20% low) produced a null result (consistent with simulations). With the bunchers "off", ε_x increased by $\sim 33\%$ at the M3-exit (dispersion in the bend plane), and by a factor of 3 at the M4-exit (due to beam debunching), but ε_y remained unchanged, as expected. Large emittance growth (in ε_x and ε_L) was observed for improper phasing of the deflector (Figures 3A and 4A).

Figure 5 shows ε_L as measured after a ~ 35 cm drift and at the exits of the DTL, M1-, M3-, and M4-plates. Using the DTL design ε_L as input to simulations, an upper limit of $\sim 5\%$ ε_L growth through the funnel is predicted. The observed growth was ~ 15 to 20%. The error on ε_L is a few percent ($\sim 5\%$) and reflects the scatter in the measured values. The results for non-optimum buncher operation were basically the same. The measured ε_L of the DTL output beam was ~ 4 times smaller than the design value of ε_L, so even a 20% emittance growth through the funnel was not detrimental to the funnel's performance.

The major objectives of the ATS single-beam funnel were realized. Position (i.e., steering) control was achieved throughout the funnel with a $\sim 100\%$ beam transmission. The use of rf deflection was successful. The beam-beam interaction has been shown to be negligible.[7] It deflects the beam, at most, a few tens of microradians in the deflector section of the funnel. The dependencies of beam deflection, ε_x and ε_y, the horizontal Courant–Snyder parameters, and ε_L on deflector amplitude and phase were as expected. The desired amplitude and phase set-points were easily determined. Transverse and longitudinal emittance growth through the ATS single-beam funnel was controlled. As expected, no transverse emittance growth was observed, within experimental precision. Non-optimum operation of the rf bunchers also failed to produce any measureable transverse emittance growth. Longitudinal emittance growth through ATS single-beam funnel was controlled to a level that was not detrimental to the funnel's performance. A measurement of longitudinal emittance growth in a drift (~ 35 cm) showed large growth (60–80%). Transverse and longitudinal emittance control in the funnel beamline (length ~ 160 cm) has eliminated this large growth (Figure 5).

The successful completion of the ATS single-beam funnel experiment would not have been possible without the cooperation of many individuals throughout the Accelerator Technology Division of LANL.

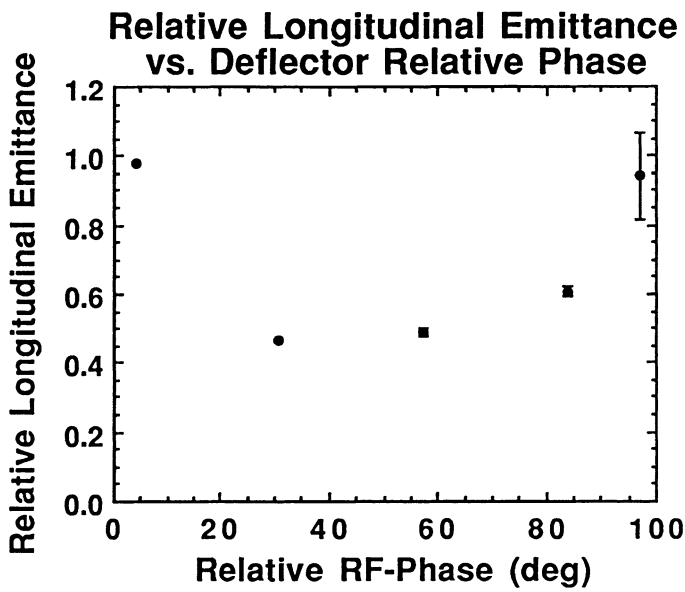

A

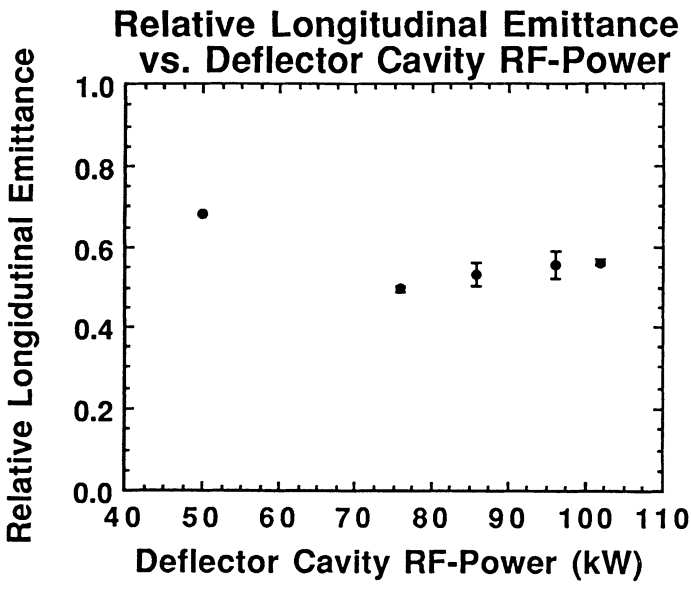

B

FIGURE 4 (A) Relative ε_L vs. relative deflector phase. Deflector cavity power set at 86 kW. (B) Relative ε_L vs. deflector cavity power. Design gap voltage (333 kV) occurs at 86 kW.

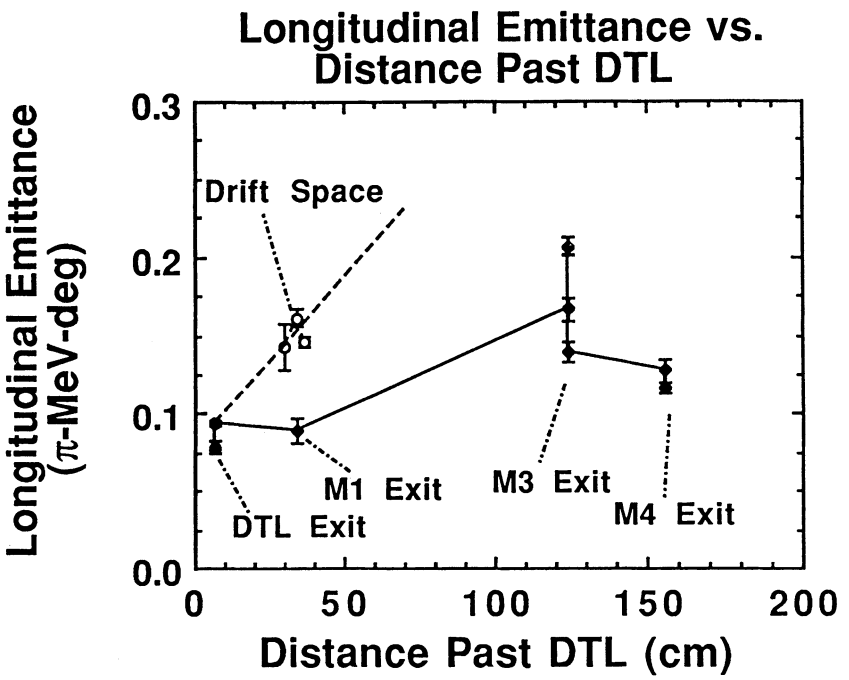

FIGURE 5 Shown is ε_L as measured (for optimum buncher settings) after a $\sim$35-cm drift and at the exits of the DTL, M1, M3, and M4 plates. The large scatter in the data sets at the M3 exit are partially attributed to changes in the beam phase spread. The lines are to guide the eye.

REFERENCES

1. O. R. Sander, *et al.*, Los Alamos National Laboratory report LA-CP-89-489 (July 1989).
2. R. J. Kashuba, *et al.*, Los Alamost National Laboratory report LA-CP-89-277 (July 1989).
3. W. B. Cottingame, *et al.*, Proc. 1985 Particle Accelerator Conference, *IEEE Trans. Nucl. Sci.* **32**(5), 1871 (1985).
4. C. M. Fortgang, *et al.*, Proc. 1988 Linear Accelerator Conference, Continuous Electron Beam Accelerator Facility CEBAF-Report-89-001 (June 1989), p. 167.
5. J. D. Gilpatrick, *et al.*, Proc. 1988 Linear Accelerator Conference, Continuous Electron Beam Accelerator Facility CEBAF-Report-89-001 (June 1989), p. 134.
6. G. O. Bolme, *et al.*, *Proc. 1990 Linear Accelerator Conference*, September 10–14, 1990.
7. F. W. Guy, "Beam-Beam Interaction in High-Current Ion Funnels," Los Alamos National Laboratory memorandum AT-1:90–104.